

Regional Geoid Modelling

Khushbu, Mohammed Iqlash

1. Abstract

We employed the classical remove-restore method to estimate a regional geoid across a $3^\circ \times 6^\circ$ area in Texas, USA. This involved several steps, including the reduction of normal gravity, application of free air correction, correction for atmospheric attraction, adjustment for long-wavelength gravity anomalies, and terrain correction. These corrections were applied to observed air-borne gravity values. Subsequently, we restored long-wavelength undulation and considered the indirect effect using the Bruns formula to calculate undulation.

2. Introduction

The primary objective of physical geodesy is to achieve precise determination of the geoid at a centimeter level, aligning with the accuracy of GPS height determination. The geoid serves as an equipotential surface for Earth's gravity field and roughly corresponds to mean sea level. The geoid exhibits irregularities due to the Earth's rotation and variations in mass distribution. Its form is defined by the undulation height (N) in relation to a global reference ellipsoid. Geoid undulation spans from +85 meters near Iceland to -106 meters in Southern India. A geoid model and its temporal variations facilitate exploring and understanding diverse natural phenomena, encompassing the Earth's interior structure and dynamic processes such as hydrological mass changes, glacier melt, isostasy, and more.

The primary objective of physical geodesy is to achieve precise determination of the geoid at a centimeter level, aligning with the accuracy of GPS height determination. The geoid serves as an equipotential surface for Earth's gravity field and roughly corresponds to mean sea level. The geoid exhibits irregularities due to the Earth's rotation and variations in mass distribution. Its form is defined by the undulation height (N) in relation to a global reference ellipsoid. Geoid undulation spans from +85 meters near Iceland to -106 meters in Southern India. A geoid model and its temporal variations facilitate exploring

and understanding diverse natural phenomena, encompassing the Earth's interior structure and dynamic processes such as hydrological mass changes, glacier melt, isostasy, and more.

The geoid height can be determined from measurements of gravity acceleration on the Earth; specific satellite missions like CHAMP, GRACE, and GOCE have been executed to achieve global coverage in gravity surveys. While satellite-based gravity observations offer a spatial resolution of 100 km, practical applications often necessitate a much higher-resolution geoid. Airborne gravity surveys are conducted to address this need, enhancing accuracy and spatial resolution. Despite the unavailability of airborne gravity data for the globe, they are employed to derive high-resolution regional geoids.

In order to obtain geoid undulations using gravity data, the traditional remove-restore method is used. In the remove-restore method, the effect of the topographic-isostatic masses is removed from the source gravitational data. Then, undulations due to each component, i.e., long wavelength, small wavelength, and indirect effects due to terrain, are restored to the resulting geoidal heights. In order to obtain the undulation due to slight wavelength, gravity anomaly is obtained using the Stokes integral. However, since it is computed over the entire globe and the data for the entire globe is not available, this truncation of the area causes an error in the geoid computation. For handling, this truncation of the Stokes global integral into a limited spherical cap radius and modifying the Stokes' kernel are often used.

3. Methodology

3.1. Gravity Corrections

Following reductions have been performed on gravity field to convert it to free gravity anomalies.

■ The Normal Gravity values

$$\gamma = \frac{a\gamma_a \cos^2(\Phi) + b\gamma_b \sin^2(\Phi)}{\sqrt{a \cos^2(\Phi) + b \sin^2(\Phi)}} \quad (1)$$

where a and b are the semi-major and semi-minor

axes of reference ellipsoid, γ_a and γ_b are the normal gravity values at the equator and at the poles, respectively and Φ is the geodetic / ellipsoidal latitude. For WGS84 ellipsoid $a = 6378137$ meters, $b = 6356752.3142$ meters $\gamma_a = 978032.53359$ m/s^2 and $\gamma_b = 983218.49378$ m/s^2 .

- **Free air reduction & free air anomaly**

$$FAA = 0.3086 \times H \quad (2)$$

Here H is the Orthometric height in meters. The free air gravity anomaly can be calculated as

$$\Delta g = g_{\text{observed}} + \delta g_{\text{FA}} - \gamma \quad (3)$$

- We want to reduce the long wavelength effect, thus remove the effect of a global gravity field model, a long wavelength gravity anomaly (Δg_{GGM}). After its removal the resultant **reduced gravity anomaly** only contains the medium and small wavelengths. For our Study area we use GGM05 model.

$$\Delta g_{\text{smw}} = \Delta g - \Delta g_{\text{GGM}} \quad (4)$$

- **Atmospheric correction** to account for gravitational attraction of atmosphere is given as follows,

$$\delta g_{\text{atm}} = 0.871 - 1.0298 \times 10^{-4}H + 5.3105 \times 10^{-9}H^2 - 2.1642 \times 10^{-13}H^3 + 9.5246 \times 10^{-18}H^4 - 2.2411 \times 10^{-22}H^5 \quad (5)$$

- Now we need to do **terrain correction** or the gravitational effect of topography. At a given point P, the terrain correction could be evaluated using:

$$\delta g_T = \frac{G\rho}{2} [(H_P)^2 (\mathcal{F}^{-1}(\mathcal{F}(1)\mathcal{F}(1/r_Q^3)) + (\mathcal{F}^{-1}(\mathcal{F}(H_Q^3)\mathcal{F}(1/r_Q^3)) - 2H_P(\mathcal{F}^{-1}(\mathcal{F}(H_Q)\mathcal{F}(1/r_Q^3))]) \quad (6)$$

Where H_P and H_Q are heights of the evaluation and data points respectively and

$$r = \sqrt{(x_P - x_Q)^2 + (y_P - y_Q)^2 + (z_P - z_Q)^2}. \mathcal{F}$$

and \mathcal{F}^{-1} are the forward(analysis) and the inverse fourier transforms.

Faye Anomaly is calculated by removing δg_{atm} and δg_T from the small and medium wavelength gravity anomaly.

$$\Delta g_{\text{faye}} = \Delta g_{\text{smw}} - \delta g_{\text{atm}} - \delta g_T \quad (7)$$

3.2. Disturbing Potential

The disturbing potential is the product of small wavelength geoid undulation and normal gravity values.

$$N_r = \frac{T_r}{r} \quad (8)$$

Where T_r can be evaluated using stokes integral, where $S(\psi)$ is the stokes kernel.

$$T_r = \frac{R}{4\pi} [(\mathcal{F}^{-1}(\mathcal{F}(\Delta g_{\text{faye}})\mathcal{F}(S(\psi)))] \quad (9)$$

In closed form, the stokes kernel is given by the formula

$$S(\psi) = \frac{1}{\sin(\psi/2)} - 6(\psi/2) + 1 - 5\cos(\psi) - 3\cos(\psi)\ln(\sin(\psi/2) + \sin^2(\psi/2)) \quad (10)$$

$S(\psi)$ is the unmodified stokes kernel, ψ is the spherical distance, it is computed as a function of the spherical coordinates (latitude ϕ_P and longitude λ_P) of the computation point and the coordinates (ϕ_Q , λ_Q) of the data points.

$$\sin^2(\psi/2) = \sin^2\left(\frac{\phi_P - \phi_Q}{2}\right) + \sin^2\left(\frac{\lambda_P - \lambda_Q}{2}\right)\cos(\phi_P)\cos(\phi_Q) \quad (11)$$

3.3. Restoring the Geoid

By using the Brun's formula, we calculate the small wavelength geoid undulation. Further, we calculate the co-geoid by adding long wavelength undulations corresponding to the GGM05 global field model.

$$N_{\text{cogeoid}} = N_r + N_{\text{GGM}} \quad (12)$$

The geoid can be computed by adding the indirect effect of the corresponding gravity terrain correction (δg_T) to the co-geoid.

$$N_{\text{geoid}} = N_{\text{cogeoid}} + \delta N_{\text{indirect}} \quad (13)$$

we are not dealing with the $\delta N_{\text{indirect}}$.

4. STUDY AREA AND DATA

Air-borne gravity and elevation data provided by NOAA's National Geodetic survey, "Gravity for the redefinition of the American Vertical Datum", or GRAV-D was used. The study area was $3^\circ \times 6^\circ$ ranging between -102° E, 30° N to -96° E, 33° N, lying in Texas, USA. The study area consisted of 1,35,955 points. We used long wavelength undulation and long wavelength gravity anomaly from the GGM05C model, made available by ICGEM, was used to estimate the orthometric height and short medium wavelength gravity anomaly. Height data from SRTM Digital Elevation Model, provided by CGIAR-CSI was used to calculate terrain correction.

5. Implementation

5.1. Reduction

The observed gravity values from our data are reduced to faye anomalies in following steps:

Normal gravity and free air correction computed using equation (1) and (2) respectively for all data points. These are removed from observed gravity values to give free air gravity anomaly Δg .

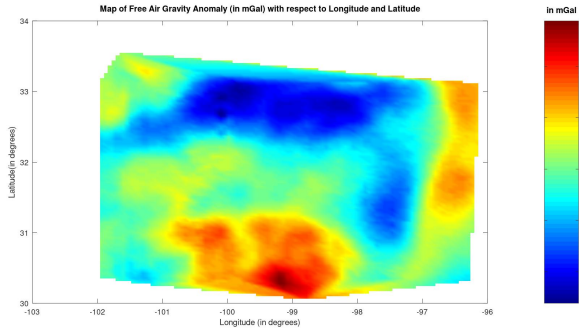


Figure 01: Free Air gravity Anomaly Δg_{FA}

Long wavelength gravity anomaly Δg_{GGM} from the GGM05 model and correction due to atmospheric attraction δg_{atm} are reduced from free air gravity anomaly. The resultant reduced gravity $\Delta g_{atm\ smw}$ at 135955 data points is interpolated to 100×100 points in a grid.

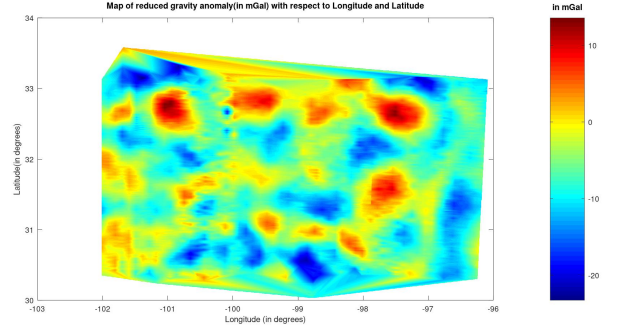


Figure 02: Reduced gravity Anomaly Δg_{smw}

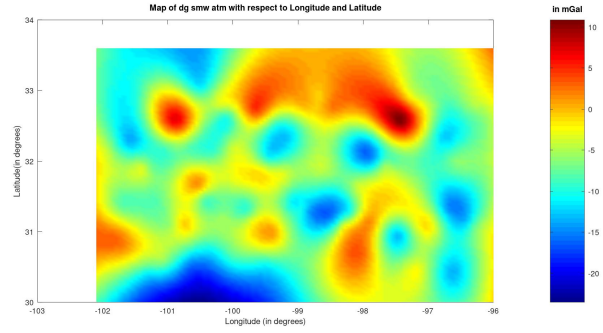


Figure 03: smw and atmospheric corrected gravity Anomaly $\Delta g_{smw\ atm}$

Terrain correction is calculated using heights from SRTM over our study area with a resolution of 1 arc second.

$$\delta g_T = \frac{G\rho}{2} [(H)^2 (\mathcal{F}^{-1}(\mathcal{F}(1)\mathcal{F}(W/r_Q^3)) + \{\mathcal{F}^{-1}(\mathcal{F}(H^3)\mathcal{F}(W/r_Q^3) - 2H(\mathcal{F}^{-1}(\mathcal{F}(H)\mathcal{F}(W/r_Q^3))]$$

Where H is the height from DEM, r is the euclidean distance and W is the kernel weighting function. r is calculated with respect to the center point of the grid. For our study, we have taken $W = 1$. δg_T is calculated and it is removed from reduced gravity anomaly, to estimate Δg_{faye}

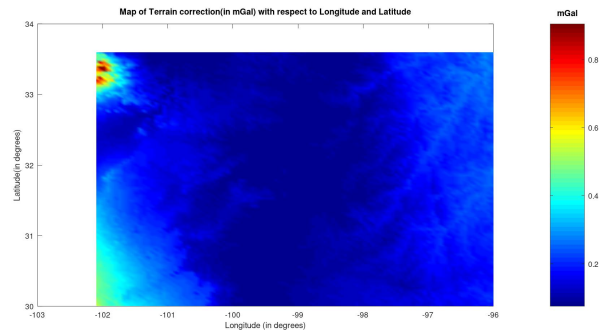


Figure 04: Terrain correction Δg_T

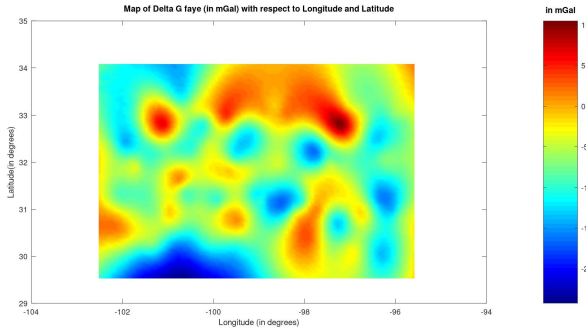


Figure 05: Faye Anomaly Δg_{faye}

5.2. Restoration

Now the reduced faye gravity anomaly are used to calculate geoid. Disturbing potential T_r is calculated using equation (9) and (10). It is used to calculate the small and medium wavelength component of disturbing potential.

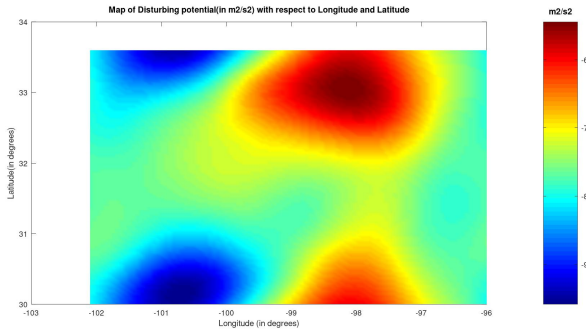


Figure 06: Disturbing potential T_r

Small wavelength geoid undulation is estimated with the help of Brun's formula, equation (8).

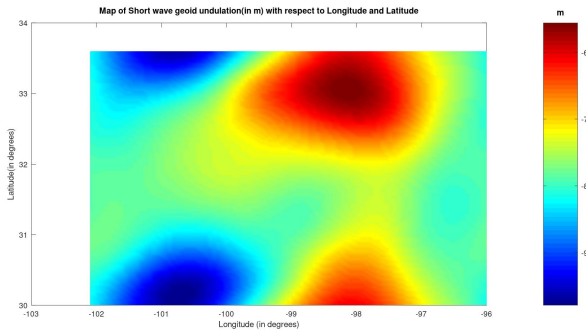


Figure 07: Short wave geoid undulation N_r

After adding the long wave length geoid undulation downloaded from GGM05 model in short

wavelength geoid undulation, we can get N_{cogeo}

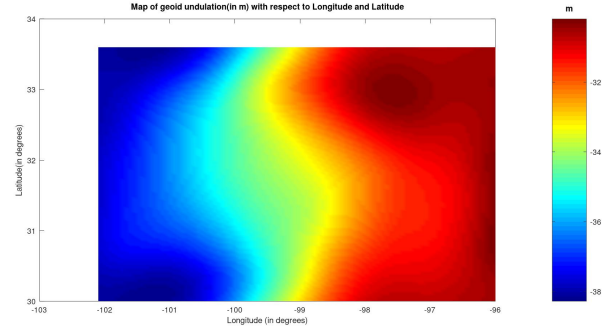


Figure 08: Estimation of cogeo N_{cogeo} T_r

6. Referencias

- Hussein Abd-Elmotaal and Nobert Kuhnreier. "An Attempt Towards an Optimum Combination of Gravity Field Wavelengths in Geoid Computation". (In: vol. 133. Jan. 2008, pp. 203-209. ISBN: 978-3-540-85425-8. DOI: 10.1007/978-3-540-85426-5_24.)
- Team GRAV-D. "Gravity for the Redefinition of the American Vertical Datum (GRAV-D) Project, Airborne Gravity Data; Block MS01". In: (2018). <https://www.noaa.gov/>.
- J. C. McCubbine et al. "Gravity anomaly grids for the New Zealand region". In: New Zealand Journal of Geology and Geophysics 60.4 (2017), pp. 381-391. DOI: 10.1080/00288306.2017.1346692. eprint: <https://www.tandfonline.com/doi/full/10.1080/00288306.2017.1346692>
- Rene Forsberg. "Gravity field terrain effect computations by FFT". In: Bulletin geodésique 59 (1985), pp. 342-360. <https://link.springer.com/article/10.1007/BF02521068>
- Will Featherstone. "Band-limited Kernel Modifications for Regional Geoid Determination Based on Dedicated Satellite Gravity Field Missions". In: (Jan. 2002). https://www.researchgate.net/publication/251367689_Band-limited_Kernel_Modifications_for_Regional_Geoid_Determination_Based_on_Dedicated_Satellite_Gravity_Field_Missions
- C. Hirt. "Mean kernels to improve gravimetric geoid determination based on modified Stokes's integration". In: Computers

Geosciences 37.11 (2011). Geospatial Cyberinfrastructure for Polar Research, pp. 1836–1842. ISSN: 0098-3004. DOI: <https://doi.org/10.1016/j.cageo.2011.01.005>. URL: https://www.researchgate.net/publication/220164181_Mean_kernels_to_improve_gravimetric_geoid_determination_based_on_modified_Stokes's_integration

- E. S. Ince et al. “ICGEM – 15 years of successful collection and distribution of global gravitational models, associated services, and future plans”. In: Earth System Science Data 11.2 (2019), pp. 647–674. URL: <https://www.sciencedirect.com/science/article/pii/S1674984721000033>